School of Physics and Astronomy

Longitudinal spin fluctuations in Heisenberg magnets

Career Development Summer Scholarship Project

Report

Alex Richardson

Contents

1 Introduction

The Classical Heisenberg model of magnetism is a simple yet effective model that accurately predicts properties of ferromagnetic materials. It allows for exploring the phase transition between ferromagnetic and paramagnetic behaviour as the temperature varies, as well as allowing anti-ferromagnetism and helimagnetism. The Classical Heisenberg model achieves this only by allowing transverse spin fluctuations (spin vectors can change direction), but the modelling of some materials require longitudinal fluctuations (allowing the spin vectors to change magnitude). The more general Heisenberg-Landau model incorporates this, by including an on site potential that limits the size of longitudinal fluctuations. Typically, parameters of the Heisenberg-Landau model are found for a specific material, through quantum mechanical calculations from first principles (like DFT). The model is then used to make predictions about the thermodynamic properties of this material. In this regard, the Heisenberg-Landau model is very useful. However, the general behaviour of the model is not well understood.

The aim of this project was to investigate the general behaviour of the Heisenberg-Landau model, in particular, how the thermodynamic properties vary with the potentials that constrain longitudinal fluctuations. A toy model, with an on site potential dependant on one parameter was used, on a cubic lattice. The formation of spin structures and the effects of both direct and Dzyaloshinskii–Moriya (DM) interactions were also explored. This was all done by implementing Monte Carlo heat bath simulations of the models in C++.

1.1 Lay Summary

The Classical Heisenberg model of magnetism is a simple but useful model, defining a grid of interacting magnetic atoms. By defining how neighbouring atoms interact, emergent behaviour can be measured. From this, properties of real materials can be calculated. The Heisenberg-Landau model is a generalisation of the Classical Heisenberg, and although it is subtly different in definition, it allows for quite different behaviour. It is, in general, more powerful and accurate. This model is frequently used, by fitting some parameters with purely quantum mechanical calculations, to predict the properties of real materials in a variety of conditions. However, general behaviour of the model is not well understood, especially as one gradually changes from the Heisenberg-Landau to the Classical Heisenberg. The aim of this project was to investigate this general behaviour, by simulating a simplified material on a computer. The formations of magnetic structures in the material were also explored.

1.2 Personal Statement

Whilst doing this project I developed a lot of useful skills. On the technical side, I learned how to write and debug C++ and how to use Bash scripts, as well as how to schedule jobs on a powerful parallel computing cluster. On the non-technical side, I got experience in working in an academic environment, where I learned how to communicate with experts on highly specific and technical subjects. I offered my own ideas and worked fairly independently, but met my supervisor weekly to check everything was on schedule. I developed my scientific report writing skills, and learned how to condense a project down to an academic poster. I refined my public speaking as I presented the poster to a group of lecturers and PhD students. I improved my verbal communication skills in attempting to explain my project work to my peers, both physics students and laymen.

2   Method

2.1   Models

4 different models of ferromagnetism are briefly presented here, some of which are generalisations of the others. All of these models are defined on a lattice of strongly interacting spins. The lattice can be of any shape or dimension, although all the simulations here were run on cubic lattices with periodic boundary conditions. Next nearest neighbour terms were included as in [1], to enable comparison of results.

2.1.1   Ising

The simplest model of ferromagnetism, the Ising model defines spins as either up or down. Although not used in this project, all the models that were used are generalisations of this, so it is included here for completeness. The Hamiltonian for the Ising model is:

$$H = -\frac{1}{2} \sum_{i \neq j} J_{ij} m_i m_j \tag{1}$$

m_i represents the spin on site i, and can be ± 1. J_{ij} represents the direct exchange interaction between sites i and j. If $J_{ij} > 0$, it is energetically favourable for spins i and j to align (ferromagnetism). If $J_{ij} < 0$, anti-alignment is favourable (anti-ferromagnetism). If $J_{ij} = 0$, there is no interaction between these two sites. This is the case for most sites that aren't lattice neighbours.

2.1.2   Ising-Landau

By relaxing the rule of the spins only taking two values (allowing longitudinal spin fluctuations), the Ising-Landau model is formed. Now m_i can take any real value. The hamiltonian is:

$$H = -\frac{1}{2} \sum_{i \neq j} J_{ij} m_i m_j + \sum_i u(m_i) \tag{2}$$

The symbols have the same meanings as in the Ising model, except that $m_i \in \mathcal{R}$, and the local potential $u(m_i)$ has been introduced. This potential constrains the possible/likely values of m_i by making some of them energetically unfavourable. The general form of this potential and a graph are shown below:
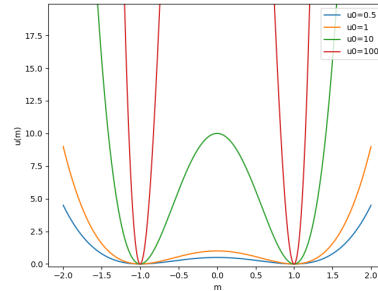
$$u(m) = u_0 \left[1 - 2m^2 + m^4 \right] \tag{3}$$

Figure 1: Potential $u(m)$ for various u_0. As u_0 increases, the possible values of m become constrained around ± 1. The limit as $u_0 \to \infty$ is the Ising model.

2.1.3 Heisenberg

The Heisenberg model differs from the Ising model by having vector spins, but of unit length (transverse fluctuations are now allowed). The hamiltonian is:

$$H = -\frac{1}{2} \sum_{i \neq j} J_{ij} \mathbf{m}_i \cdot \mathbf{m}_j \tag{4}$$

This has similar behaviour to the Ising model, except that alignment and anti-alignment are along vectors. However, vector spins allow for DM interactions to be included:

$$H = -\frac{1}{2} \sum_{i \neq j} \left(J_{ij} \mathbf{m}_i \cdot \mathbf{m}_j + \mathbf{D}_{ij} \cdot (\mathbf{m}_i \times \mathbf{m}_j) \right) \tag{5}$$

Where $\mathbf{D}_{ij}$, the DM exchange parameter, is a vector pointing from site i to site j on the lattice. The magnitude of this vector controls the strength of the interaction. Values between 0 and 1 are typically used, and $\mathbf{D}_{ij} = 0$ for any non neighbouring lattice points. The cross product between neighbouring spin vectors is minimised when they are perpendicular. This, competing with the direct exchange being minimised when spins are aligned, can produce more complex stable spin structures.

2.1.4 Heisenberg-Landau

By allowing the vector spins to take any magnitude, the Heisenberg model is generalised to the Heisenberg-Landau. The hamiltonian is:

$$H = -\frac{1}{2} \sum_{i \neq j} J_{ij} \mathbf{m}_i \cdot \mathbf{m}_j + \sum_i u(\|\mathbf{m}_i\|) \tag{6}$$

Here the local potential $u(\|\mathbf{m}_i\|)$ is the same as $u(m)$ from the Ising-Landau model, but it constrains the possible/likely values of the magnitude of the spin vectors. Like with the Ising-Landau model, as u_0 approaches infinity, the Heisenberg-Landau model becomes the Heisenberg model. A particular focus of this project was gradually varying u_0 and seeing how this affected thermodynamic properties of the simulated magnets. By including the DM interactions, the most general model of magnetism used here is formed:

$$H = -\frac{1}{2} \sum_{i \neq j} \left(J_{ij} \mathbf{m}_i \cdot \mathbf{m}_j + \mathbf{D}_{ij} \cdot (\mathbf{m}_i \times \mathbf{m}_j) \right) + \sum_i u(\|\mathbf{m}_i\|) \tag{7}$$

2.2 Monte Carlo Heat Bath algorithm

The Heat Bath algorithm used is a form of Monte Carlo algorithm. Most of what was done for this project was based on [3]. It is conceptually very similar to the more standard Metropolis-Hastings algorithm. The only difference (in implementation) is that, where the Metropolis algorithm accepts or rejects spin updates based on how much they change the energy, the Heat Bath algorithm always accepts spin updates, but drawn from a probability distribution defined by local interactions.

The reason for using the Heat Bath over the Metropolis algorithm is that changes in spin are very likely to increase the total energy, so are likely to be rejected by Metropolis. This would require a large number of update attempts to bring the system to equilibrium. The Heat Bath algorithm avoids this issue, but at the cost of having to perform some numerical integrals to approximate the probability distribution from local spins. A pseudo-code Heat Bath algorithm is presented below:

```
Total Energy ← 0
initialise spins
for i ← 0 to sweeps do
    for j ← 0 to N do
        /Choose random site and compute local field
        (x, y, z) ← random lattice site
        old spin ← spins[x, y, z]
        h ← local field(x, y, z)
        /Update spin from probability distribution
        new spin ← distribution(h)
        /Compute energies
        E₁ ← − old spin · h + u(‖old spin‖)
        E₂ ← − new spin · h + u(‖new spin‖)
        ΔE ← E₂ − E₁
        /Store energy change
        Total Energy ← Total Energy + ΔE
        /Update spin
        spins[x, y, z] ← new spin
    end
    if i >eq sweeps then
        write data
    else
    end
end
```

Where N is the number of lattice sites, $local\ field()$ returns the magnetic field due to neighbouring spins, and $distribution()$ returns a random spin drawn from a probability distribution defined by the local field. The details of how these 2 functions work vary widely depending on which model is implemented. For Heisenberg models, the multiplications when assigning E_1 and E_2 are dot products. $spins$ is a 3D array of spin values at each lattice site (4D array in the case of vector spins).

In practice, the initial random $spins$ state is nowhere near the equilibrium state, so the system has to run for a while before any meaningful results can be extracted. This is the reason for the if statement containing $write\ data$, so that data is only written once a set number of sweeps has been completed. Typically, the total number of sweeps used was 20,000, and the number of equilibrating sweeps (before data was measured) was 10,000. Sweeps after the system is in equilibrium will be referred to as measurement sweeps, although the system is still being simulated.

Temperature comes into these simulations in the $local\ field()$ and $distribution()$ functions. However, running a simulation at only one temperature is not particularly interesting. The simulations were started at a high temperature, with $spins$ initialised randomly. Then the final state of $spins$ after a full set of $sweeps$ was used as the input state to the next simulation, at a slightly lower temperature. This was repeated, until the temperature reached 0, or low enough. This allows for investigating temperature dependant phase transitions.

2.3   Implementation

A C++ program simulating the Ising-Landau model was provided by Harry Keen, I then generalised it to simulate both Classical Heisenberg and Heisenberg-Landau models. This was not a trivial generalisation, but the details are not worth discussing in length. For a full history of the development, see the GitHub link (https://github.com/AlexDR1998/Heisenberg-Spins). All of the data analysis and visualisation was done with Python (extensive use of Numpy and MatPlotLib). The bulk of these

simulations were run on EDDIE, a University of Edinburgh research computing cluster. This required tying together the C++ simulations with bash scripts. This allowed some fairly naive but effective parallelism to be exploited, as many simulations had to be run with subtly different parameters. Again see the GitHub link for details.

2.4   Extracting thermodynamic properties

The three main sets of data given by the simulations are: The mean (over measurement sweeps) spin per site, the mean (over all sites and measurement sweeps) energy, and the mean of the squares of energies (over all sites and measurement sweeps). The mean (over measurement sweeps) of the squares of the spin per site, and the mean (over all sites and measurement sweeps) spin were also returned, but they were not used as much.

The most commonly used thermodynamic property here was Heat Capacity, as it diverges to infinity (in the thermodynamic limit) at a ferromagnetic phase transition. This could be calculated from the energy outputs in two ways:

$$C = \frac{1}{kT^2}(\langle E \rangle^2 - \langle E^2 \rangle) \tag{8}$$

$$C = \Big(\frac{\partial \langle E \rangle}{\partial T}\Big)_{v,p} = \frac{d\langle E \rangle}{dT} \tag{9}$$

Where the partial derivative is keeping pressure or volume constant. As both pressure and volume are not explicitly included in the simulations, they are assumed as constant. The first method is derived from statistical mechanics, the second from classical thermodynamics. Reassuringly they both give the same results, again confirming the equivalence of statistical mechanical and thermodynamic definitions of heat capacity. However in some situations one may give slightly noisier results, so there is no clear best method.
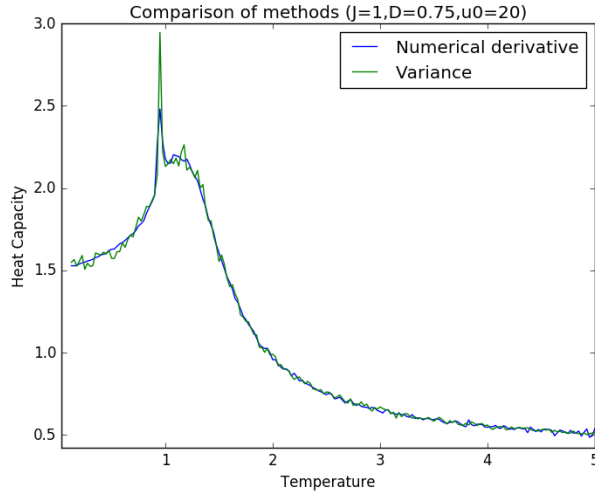

Figure 2: Comparison of different methods of calculating heat capacity

The variance method does allow for calculating the heat capacity for any single temperature, without having to calculate at neighbouring temperatures, however the derivative method only requires the mean energy.

6

3   Results

3.1   Heat Capacities

The heat capacities for a set of u_0 values were computed on a 24*24*24 cubic lattice. For readability, only a few are superimposed, although all the graphs have the same form. This was done for both purely ferromagnetic ($J = 1, D = 0$) and with DM interactions ($J = 1, D = 0.75$). The specific value $D = 0.75$ was used to compare results with [1,2]. A Classical Heisenberg heat capacity is also included in each plot for comparison, although it does naturally converge to a lower 0 temperature heat capacity.
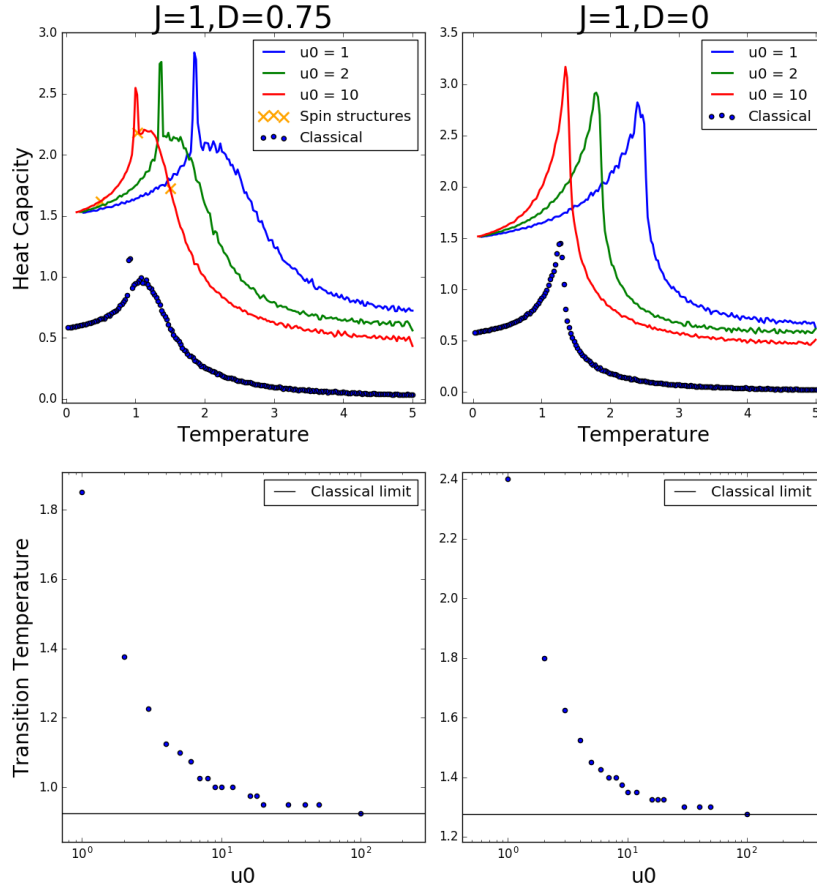

Figure 3: Heat capacities and transition temperature plots for ferromagnetic and mixed (ferromagnetic with DM) systems. Points marked with X's correspond to the spin structures included in Figure 4 . Horizontal lines give Classical Heisenberg limits of transition temperature.

To calculate the transition temperatures, a peak finding algorithm was used. It was fairly basic, as each heat capacity plot had only one peak. In both the purely ferromagnetic case, and with DM interactions, the transition temperatures approach the Classical Heisenberg limit from above as u_0 is increased. These were produced with the numerical derivative method. The ($J = 1, S = 0$) transition temperature plot disagrees with [2]. Stishov and Belemuk find that the transition temperatures fall below the Classical limit and approach from below. This plot also disagrees with Harry Keen's as yet unpublished exploration of the Ising and Ising-Landau model. The reason for this is not understood, it is possibly a bug, but only subtly emergent one. The $J = 1, D = 0.75$ results agree with the literature.

3.2   Spin Structures

As the direct (ferromagnetic) and DM interactions compete to minimise the energy in different ways, there are some interesting spin structures forming at equilibrium.
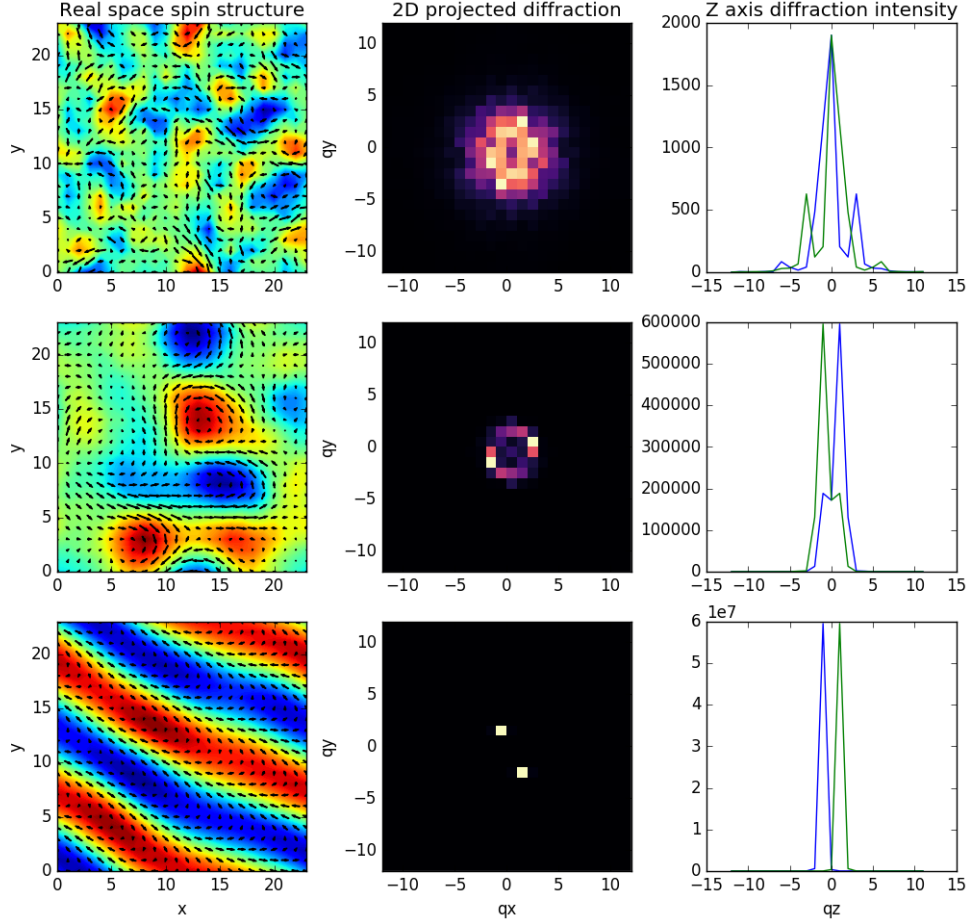

Figure 4: From top to bottom: above, at and below phase transition ($J = 1, D = 0.75, u_0 = 10$)

On the left are 2D slices of the real space spin structures. Arrows indicate spin components in the xy plane, whilst colour indicates z components (green being roughly 0).

In the middle are diffraction patterns produced using Fourier Transforms of the spin data, roughly simulating a diffraction experiment. The spin data is split into Cartesian components, giving 3 scalar data sets in 3D. Each of these is processed with a 3D Fourier Transform, and the 3 sets of results are combined by calculating the vector magnitudes, giving one 3D data set. The 2D images are produced by summation along the z axis of this data. Sharp non-zero peaks indicate periodic spin structures, whereas peaks at 0 indicate non-periodic structures. The images on the right show how the Fourier Transform intensity varies along the z axis, with x and y fixed at a peak. This recovers the useful information lost in flattening the data to 2D.

The spin structures in the paramagnetic phase are typically unstructured, as there is no external magnetic field applied. On the broad plateau in the $J = 1, D = 0.75$ heat capacities, vortex like structures are observed. After the sharp peak, spin structures form sinusoidal stripes. These formations were observed regardless of u_0 value, changing u_0 only shifted the temperature regions at which they were observed. They were also observed in the Classical Heisenberg model. Below are some spin structures for $u_0 = 1$:
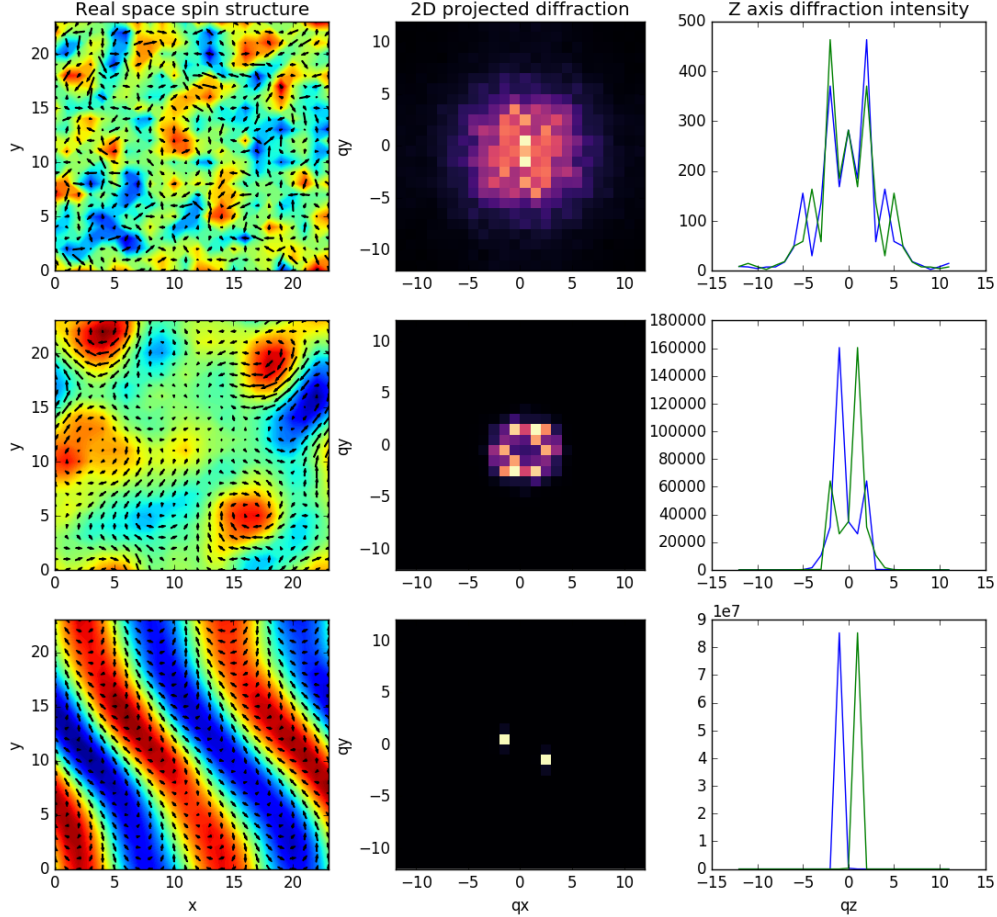

Figure 5: From top to bottom: above, at and below phase transition ($J = 1, D = 0.75, u_0 = 1$)

Qualitatively the structures had no dependence on u_0 (besides transition temperature shifting), although a more detailed analysis might reveal otherwise. It is possible that for small enough u_0 ($0 < u_0 << 1$), these spin structures might change, as energy can be minimised more easily with longitudinal fluctuations. However this is hard to explore as the computations often diverge. In the case of purely ferromagnetic simulations, the spin structures are exactly as expected, with all spins aligning below the phase transition.
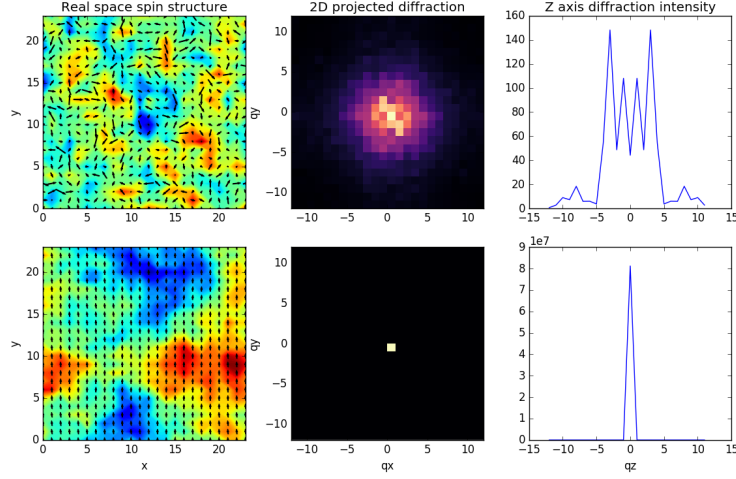
Figure 6: From top to bottom: paramagnetic phase, purely ferromagnetic phase ($u_0 = 10$)

There are of course some challenges in visualising 3D data on a 2D computer screen. The choice of where to take a 2D slice should be arbitrary, assuming no structures are oriented in a plane. Shown below are some of the same spin structures as in Figure 4, but with choice of slicing plane (xy, zx or yz planes).
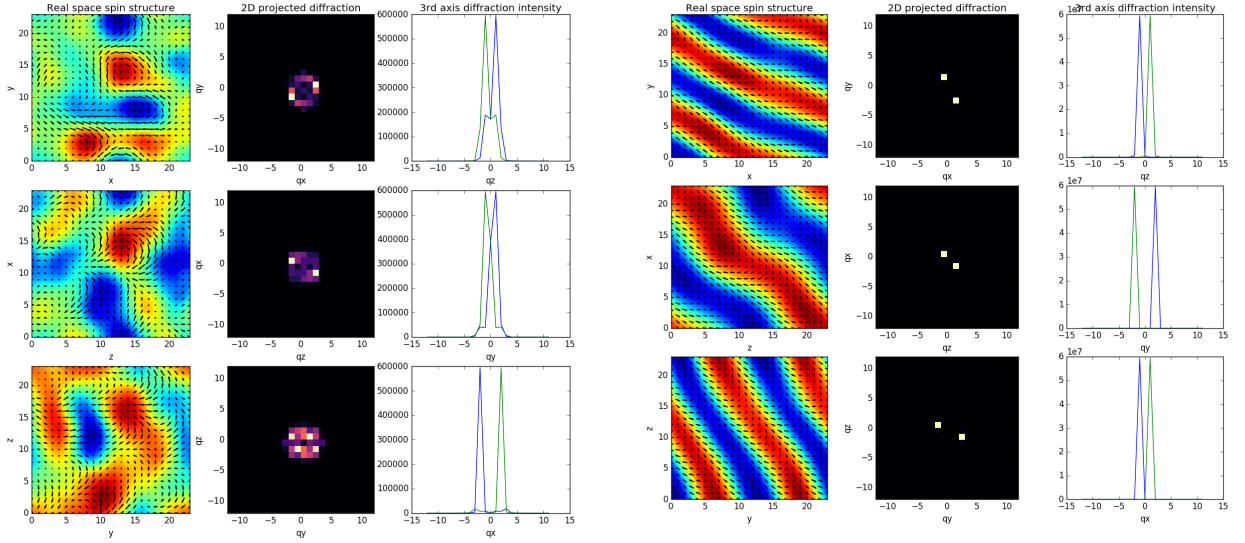
(a) At phase transition

(b) After phase transition

Figure 7: 3 possible planes of visualising spin structures ($J = 1, D = 0.75, u_0 = 10$)

The spin stripes formed after the phase transition appear fairly similar in all possible viewing planes. However, the vortex spin structures formed on the plateau of the wide phase transitions on Figure 3 vary with viewing angle (both in real and fourier space), which implies these structures align

to particular planes. It is possible that these are an artefact of the cubic lattice structure, and it should be determined if they form on different lattice shapes, although this has not been done here.

There are various other forms of visualisation possible that don't work well here, such as animations, 3D plots or 3D printed models. The code for animations and 3D plots is included in the GitHub repository, the preliminary processing for putting data into a CAD for 3D printed models is also included, although the practicalities of producing a model have not been worked out yet.

3.3   Finite lattice size effects

It is worth noting that bulk thermodynamic properties are being derived from cubic lattices with of order 10^4 lattice sites, whereas real materials have of order 10^{23} interacting atoms. The workaround is the use of periodic boundary conditions, which assumes that the material being simulated extends indefinitely and periodically in all directions. It is a fairly safe assumption here, but can lead to some effects when considering spin structures. In figure 4, there is actually just one spin stripe that wraps around the boundaries multiple times.

Initially, the simulations were done on 20*20*20 cubic lattices. This was an arbitrary choice, but the periodic spin stripes were always the results of plane waves on the [111] lattice plane. Switching to a 24*24*24 lattice was an improvement, both due to increased size and divisibility. If any periodic structure with a period that isn't a factor of the cell size forms, it will likely be distorted or destabilised. As 24 has more factors than 20, it is more likely that a periodic spin structure will not be disturbed by the periodic boundary conditions in a 24*24*24 lattice. It was found that more interesting periodic structures formed on a 24*24*24 lattice:
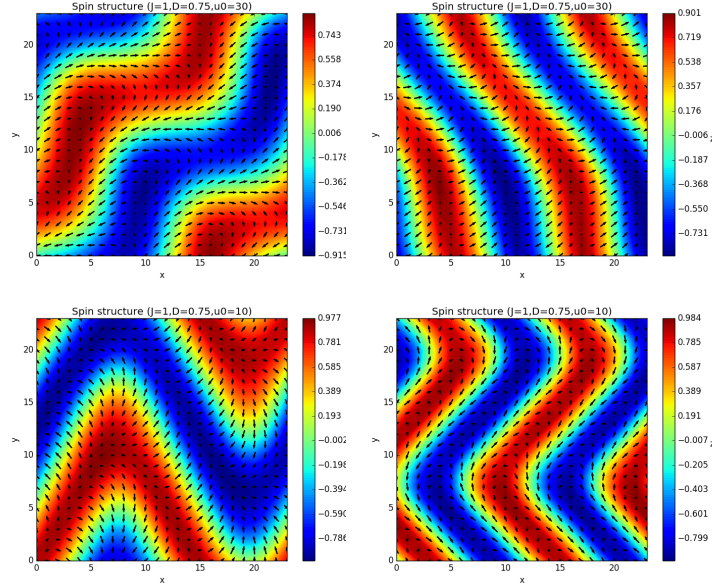

Figure 8: A variety of periodic spin structures, all below phase transitions.

In future, perhaps a few simulations on 60*60*60 cubic lattices should be performed, although at that point it might start becoming computationally intractable without using some parallel Monte Carlo techniques.

4 Conclusion

In conclusion, the temperature at which the paramagenetic to ferromagnetic (or helimagnetic) phase transition occurs in Heisenberg-Landau magnets is dependent on the strength of the on site potential. The exact nature of this dependence is not fully understood, as the results for ferromagnetism contradict the literature results we aimed to reproduce. However, in the case of increasingly large u_0, the Classical Heisenberg model is thankfully recovered. The formation of different spin structures are largely dependent on the interaction types between atoms, however the only clear dependence on the on-site potential is to shift the temperatures at which they occur.

Aside from a possible bug, the code has performed well as a demonstration of the use of the Monte Carlo Heat Bath algorithm, and could easily be used to explore other features of Heisenberg-Landau magnets. The inclusion of pressure or external magnetic fields, as well as the exploration of skyrmion phases (or other exotic spin structures) would likely be a next step.

5 Acknowledgements

References

[1] A. M. Belemuk and S. M. Stishov, Phase transitions in chiral magnets from Monte Carlo simulations, Physical Review B, **95**, 10.1103/PhysRevB.95.224433 (2017).

[2] A. M. Belemuk and S. M. Stishov, Modeling longitudinal spin fluctuations in chiral magnets, Journal of Physics Condensed Matter **31**, 10.1088/1361-648X/ab00b7 (2019).

[3] Y. Miyatake *et al*, On the implementation of the 'heat bath' algorithms for monte carlo simulations of classical heisenberg spin systems, Journal of Physics C: Solid State Physics **19**, 2539 (1986).